

Structure of a pentacene monolayer deposited on SiO₂: Role of trapped interfacial water

Songtao Wo, Binran Wang, Hua Zhou, Yiping Wang, Jonathan Bessette, and
Randall L. Headrick^{a)}

Department of Physics, University of Vermont, Burlington, Vermont 05405

Alex C. Mayer and George G. Malliaras

Department of Materials Science and Engineering, Cornell University, Ithaca, New York 14853

Alexander Kazimirov

Cornell High Energy Synchrotron Source, Cornell University, Ithaca, New York 14853

(Received 16 June 2006; accepted 17 August 2006; published online 2 November 2006)

In situ synchrotron x-ray reflectivity is used to probe the early stages of pentacene growth in real time, under conditions relevant to the fabrication of organic thin film transistors. The results reveal that there is an interfacial water layer initially present on the SiO₂ substrate and that this water layer is still present at the interface after the deposition of a pentacene thin film. The thickness of the trapped interfacial water layer does not significantly change subsequent to film deposition, even after exposure to atmospheric pressure or during vacuum annealing at 70 °C. However, a water layer is observed to form on the free surface of pentacene after sufficient exposure to water vapor, and the thickness of this layer can be reduced by subsequent vacuum annealing. These observations are correlated with organic thin film transistor mobilities measured at atmospheric pressure versus under vacuum. © 2006 American Institute of Physics. [DOI: 10.1063/1.2364565]

I. INTRODUCTION

Pentacene is one of the most promising organic semiconductors for organic thin film transistors (OTFTs) due to its high field effect mobility. Pentacene OTFTs have applications in large area electronics such as flat panel displays¹ and in ultralow-cost devices, such as sensors.² However, the results achieved vary greatly, even from one device to the next because their performance depends critically upon unknown details of the interface structure, thin film morphology, and environmental conditions.

It is generally believed that charge transport in OTFTs takes place in the first few monolayers near the interface with the gate dielectric (typically SiO₂), and the quality of the organic/dielectric interface plays a critical role in determining the field effect mobility.³ However, the mechanisms by which the environment affects the charge mobility at the buried interface between pentacene and SiO₂ are still not understood. We recently reported that an interfacial water layer is trapped between a pentacene film and a SiO₂ substrate during deposition under typical vacuum deposition conditions.⁴ One possibility is that the amount of moisture trapped at the interface varies with environmental conditions, although our results presented below suggest that this is not the dominant effect.

In this article, we report a set of experiments designed to determine the effect of interfacial water on the structural and electronic properties of pentacene thin films. First, we present x-ray reflectivity results, which show that an interfacial water layer is present even after pentacene deposition at

a substrate temperature of 70 °C. *No evidence* for a change in the thickness of the trapped water layer is found over a range of sample annealing temperatures and background pressures. However, a water layer is found to collect at the free surface of pentacene when it is directly exposed to air. Second, we report atomic force microscopy measurements, which show that the step height of the first monolayer of pentacene is significantly expanded relative to the height of the second monolayer, thus confirming the primary results of the x-ray experiments.

In a complementary set of measurements, a comparison of pentacene charge mobility is made for two types of devices: (i) devices based on the pentacene/SiO₂ interface and (ii) devices using a SiO₂ surface that has been treated with octadecyltrichlorosilane (OTS) before the pentacene deposition. OTFTs formed on OTS treated SiO₂ are known to exhibit higher charge mobility than non-OTS treated devices.^{5,6} Since OTS is highly hydrophobic and apparently prevents the formation of an adsorbed water layer, one could conclude that this is the key property of OTS that leads to this improvement.⁷ However, we find that the charge mobility in both types of devices is sensitive to environmental conditions. Thus, the combined structural and electronic results suggest that the sensitivity to environmental conditions *is not* caused by a change in the amount of moisture at the interface. Although trapped moisture at the interface plays a substantial role in device performance, sensitivity to the environment is predominantly related to condensed moisture at the free surface or at exposed grain boundaries in the film.

II. EXPERIMENT

A pentacene film was prepared in a custom-built x-ray diffraction chamber, which was mounted on a four circle

^{a)}Author to whom correspondence should be addressed; electronic mail: rheadrick@uvm.edu

spectrometer at the A2 station of the Cornell High Energy Synchrotron Source (CHESS).⁸ Specular x-ray reflectivity scans were carried out at a wavelength of $\lambda=0.1247$ nm with a 0.7% bandpass in order to determine the structure in the direction out of the plane of the film. The x-ray flux was 5×10^{12} photons/s in a 1×1 mm² beam spot. The reflected intensities were simulated using the IMD fitting package in order to obtain laterally averaged depth-resolved electron density profiles.⁹ The fitting procedure is described in more detail in Sec. III.

Pentacene was purchased from Aldrich Chemical Co. and used without further purification. Amorphous SiO₂ (thermal oxidation, about 1 μ m) was used as the substrate material. The substrates were cleaned prior to deposition in an ultrasonic bath with de-ionized water and dried with dry filtered nitrogen. Pentacene (bulk density, 1.33 g/cm³) was deposited by vacuum sublimation at 2×10^{-6} Torr and at a substrate temperature of 70 °C. The growth rate (~ 0.3 nm/min) and film thickness were measured by a quartz crystal microbalance (QCM) mounted next to the substrate. To get one monolayer accurately, growth was also monitored by x-ray reflectivity at a constant $q_z=2.04$ nm⁻¹. This is near the pentacene (001/2) anti-Bragg position, where the reflected rays from the first and second pentacene layers interfere destructively, causing the reflected intensity to decrease rapidly once the second monolayer begins to form. The growth was interrupted just as the reflected intensity reached its peak, which corresponded to a QCM reading of 1.6 nm. A regimen of temperature changes and exposure to atmospheric pressure were then carried out on the sample in order to access whether moisture can be driven away by annealing in vacuum and whether additional moisture accumulates during exposure to damp air.

The morphology of the monolayer was subsequently examined *ex situ* by atomic force microscopy (AFM) (DI 3100 Dimension microscope) in tapping mode, immediately after the completion of several x-ray reflectivity scans. Analysis of the coverage yielded a value of 1.05 ML (monolayer), in good agreement with the x-ray and QCM measurements described above. Measurements of the step height of the first and second monolayers of pentacene were also extracted from these images. A final x-ray reflectivity scan was performed in air after the completion of the AFM imaging.

Pentacene OTFTs were also prepared by vacuum deposition in a separate deposition chamber. The oxide thickness was 300 nm on a *p*-type Si substrate, and the pentacene layer thickness was 140 nm. A top contact geometry was used, where gold source and drain contacts were deposited through a shadow mask over the pentacene. A channel length of 75 μ m was used. Some samples were treated with OTS prior to pentacene deposition using a standard procedure.⁵ A Keithley model 2100 sourcemeter was used to perform *I-V* measurements on field effect transistors as a function of gate bias. Mobility values were extracted from these *I-V* curves.

III. RESULTS AND DISCUSSION

The x-ray reflectivity data obtained for the substrate and the evolution of the monolayer are shown in Fig. 1 together

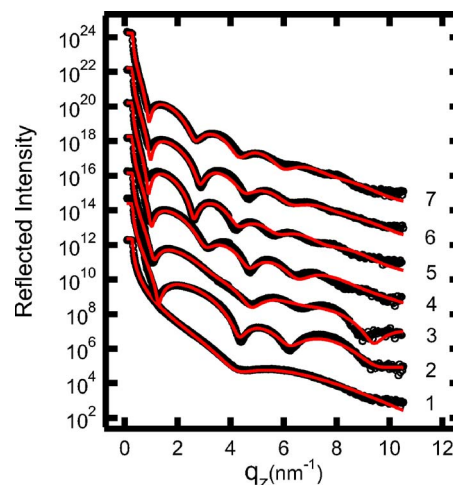


FIG. 1. X-ray reflectivity curves from 1.05 ML of pentacene on SiO₂ under different conditions, as described in the text. All of the reflectivity scans are performed in vacuum except for data sets (4) and (7), which were performed at atmospheric pressure. Successive curves have been shifted up by a factor of 100 in order to differentiate them from each other.

with simulated reflectivity curves based on a model described below. Data set (1) corresponds to the substrate before deposition, with a substrate temperature of 70 °C. The data show a broad minimum near $q_z=4.4$ nm⁻¹, which is associated with the presence of a water layer on the SiO₂ surface.

Data sets from (2) to (7) are for the same sample, but under a sequence of different conditions: (2) a fresh pentacene monolayer was deposited in vacuum at 70 °C; (3) the substrate temperature was decreased to 25 °C; (4) the sample was exposed to atmosphere for 30 min at 25 °C; (5) the exposure to atmosphere was continued for a total of 90 min; (6) the vacuum chamber was pumped back to high vacuum and the sample temperature was raised to 70 °C; (7) the sample was cooled down to 25 °C, exposed to atmosphere again, then the AFM scans were performed, and the final x-ray scan was performed after approximately 24 h of exposure.

A simple model was constructed to simulate the data sets from (1) to (7) shown as the inset of Fig. 2. In this model a “hydration layer” is introduced in order to crudely account for the structure of the pentacene/H₂O interface. The hydration layer is a general phenomenon that occurs at hydrophobic surfaces.^{10–14} It consists of a low-density water layer (“depletion layer”) with a thickness of 0.1–0.2 nm in contact with the hydrophobic surface. Since pentacene is hydrophobic, such a layer is expected to form at its interface with water. Pentacene molecules are assumed to stand vertically with respect to the plane of the substrate with almost no tilt. Also, the detailed structure of the pentacene molecule is neglected and is approximated as a uniform charge density. The layers from bottom to top are SiO₂ substrate, interfacial water (IW) layer, interfacial hydration (IH) water layer, pentacene (Pn) monolayer, top hydration (TH) water layer, and top water (TW) layer. Parameters, which are fixed in the simulations, are the densities $\rho_{\text{Pn}}=1.38$ g/cm³ (monolayer density), $\rho_{\text{IW}}=\rho_{\text{TW}}=1.00$ g/cm³, and $\rho_{\text{IH}}=\rho_{\text{TH}}=0.30$ g/cm³; the thickness of the hydration layers $t_{\text{IH}}=t_{\text{TH}}=0.15$ nm;¹¹ and the

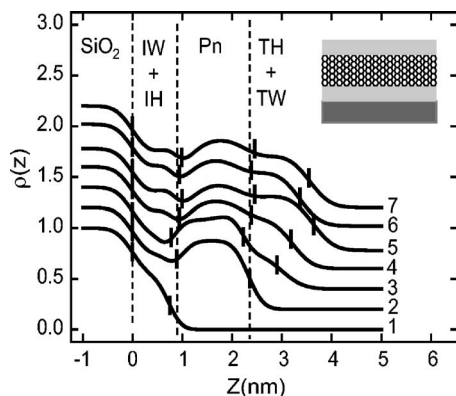


FIG. 2. Electron density profiles obtained from fitting the data in Fig. 1. The electron density is normalized to the density of the SiO_2 substrate, and each successive curve is shifted up by 0.2. The three vertical dashed lines indicate the average positions of the SiO_2 /interfacial water boundary, the hydration layer/pentacene boundary, and the pentacene/top hydration layer boundary, from left to right. The small vertical bars indicate the interface positions for each individual profile. A systematic variation of the thickness of the top water layer is apparent. The inset shows a schematic of the film structure, including the substrate, interface water layer, pentacene layer, and top water layer.

roughness of the interface water layer, $\sigma_{\text{IW}}=0.17$ nm. There are also two parameters that are coupled: $\sigma_{\text{IH}}=\sigma_{\text{Pn}}$. This is because the roughness σ_{IH} represents the roughness at the bottom pentacene/ H_2O interface, while σ_{Pn} represents the roughness of the top pentacene/ H_2O interface. We assume that the top and bottom interfaces of the pentacene layer have the same roughness.

The solid line through data set (1) in Fig. 1 is a fit to the data. A best fit for the SiO_2 density of $\rho_{\text{oxide}}=2.14$ g/cm³ and surface roughness of $\sigma_{\text{oxide}}=0.27$ nm is obtained. These values are fixed for the remaining simulations. As mentioned above, the surface has a thin layer of molecular water on it. The fit yields a thickness for the water layer of $t_{\text{IW}}=0.73$ nm, in agreement with the value obtained by Ruiz *et*

*al.*¹⁵ We note that in previous studies, we have found that the thickness of the water layer on SiO_2 (with no pentacene overlayer) is temperature dependent and that the water layer can be driven away completely during annealing in vacuum at temperatures above 100 °C.⁴

Data set (2) in Fig. 1 corresponds to the fresh pentacene monolayer right after deposition. Simulation shows an interfacial water layer between the pentacene layer and the SiO_2 substrate with a thickness of $t_{\text{IW}}=0.74$ nm. Since the thickness of the hydration layer is fixed at 0.15 nm, the sum is $t_{\text{IW}}+t_{\text{IH}}=0.89$ nm, which is the value listed in Table I. This is the total thickness of the water trapped at the interface during the deposition of the pentacene film. We use a pentacene layer thickness $t_{\text{Pn}}=1.45$ nm in order to match the period of oscillations observed in data set (2). This layer thickness is actually slightly larger than the pentacene molecular length found in the literature. For example, a length of 1.42 nm is derived from the structure results of Campbell *et al.*, while the more recent structure determination of Matheus *et al.* yields a length of 1.38 nm.^{16,17} We also find that there is no water layer on top of the fresh pentacene monolayer. However, there is a possibility that a small amount of water is present on the free surface, which might partially account for the larger than expected value of t_{Pn} . An additional factor is that the pentacene coverage is actually slightly more than 1 ML, which may also cause the measured value of t_{Pn} to be high. All of the remaining parameters extracted by fitting are listed in Table I.

Data set (3) is taken after the deposition and after cooling the substrate to room temperature and the substrate temperature has been stable for 30 min. A small shift of the first minimum in the reflected intensity towards lower q_z is observed, which reveals that the total thickness of all of the layers on top of the substrate has increased. Data sets (4) and (5) show that the total thickness continues to increase when the sample is exposed to atmosphere for 30 and 90 min,

TABLE I. Fitting parameters extracted from x-ray reflectivity. The uncertainties of the thickness values in the table are obtained by finding the range, where χ^2 is doubled in a confidence intervals calculation. The confidence intervals are estimated by computing the value of the χ^2 statistic on a grid of points in parameter space.

Condition	Temperature (°C)	Interfacial water		Pentacene		Top water	
		$t_{\text{IW}}+t_{\text{IH}}$ (nm)	$\sigma_{\text{IW}}/\sigma_{\text{IH}}^a$ (nm)	t_{Pn} (nm)	σ_{Pn}^a (nm)	$t_{\text{TH}}+t_{\text{TW}}$ (nm)	$\sigma_{\text{TH}}/\sigma_{\text{TW}}$ (nm)
1 Vacuum initial substrate	70	0.73	0.20/...
2 Vacuum fresh monolayer	70	0.89 ± 0.06	0.17/0.24	1.45	0.24
3 Vacuum cool down	25	0.76 ± 0.12	0.17/0.20	1.45	0.20	0.70 ± 0.13	0.48/0.38
4 Atmosphere exposed for 30 min	25	0.94 ± 0.12	0.17/0.34	1.45	0.34	0.81 ± 0.13	0.31/0.33
5 Atmosphere exposed for 90 min	25	0.99 ± 0.13	0.17/0.42	1.45	0.42	1.19 ± 0.14	0.31/0.33
6 Vacuum heated up	70	0.94 ± 0.12	0.17/0.41	1.45	0.41	0.98 ± 0.13	0.31/0.33
7 Atmosphere exposed for 24 h	25	0.99 ± 0.13	0.17/0.35	1.45	0.35	1.10 ± 0.14	0.31/0.33

^aThe parameters σ_{IH} and σ_{Pn} are coupled.

respectively. This change is partially reversible, as shown by data (6) taken when the vacuum chamber is again pumped out to high vacuum, and the substrate heated to 70 °C. The reflectivity data set (7) is very similar to data set (5), which implies that the total thickness of water is maximum after an exposure to atmosphere for 90 min or more, and remains stable if the humidity is constant.

In Fig. 2, the electron density profiles obtained for the different conditions are compared. For the sake of convenience, all of the electron densities have been normalized to the electron density of SiO₂ (644 e/nm³). The three vertical dashed lines indicate the nominal positions of the SiO₂/interfacial water boundary, the interfacial hydration layer/pentacene boundary, and the pentacene/top hydration layer boundary. Curve 1 shows a shoulderlike feature at $Z=0.7$ nm corresponding to the presence of the adsorbed water layer. The vertical bars on curve 1 indicate the nominal position of the substrate and water surfaces. Two additional vertical bars on each curve from 2 to 7 also indicate the position of the pentacene monolayer (between approximately $Z=0.8$ and 2.25 nm), and curves 3–7 have a fourth bar to indicate the position of the top water surface. The major difference between curve 2–7 appears at $Z>2.25$ nm, where the electron density is observed to increase when the substrate temperature decreases from 70 to 25 °C (condition 3) and continues to increase when the sample is exposed to atmosphere for 30 min (condition 4). It reaches a maximum when exposed for 90 min (condition 5). The density decreases when it is pumped back to vacuum and heated to 70 °C (condition 6). When exposed to atmosphere for 24 h (condition 7), the density associated with the water layer returns. As mentioned above, this suggests that the thickness of water layer saturates after exposure to atmosphere for 90 min. However, we emphasize that the fitting shows that it is predominantly the thickness of the top water layer that changes, while the thickness of the interfacial layer stays constant within experimental error (about 15%). The lack of an observable change in the amount of water at the interface is in contrast to the large variation of the amount of water on the free SiO₂ surface that was observed in previous studies.⁴

AFM images taken from the same sample after exposure to atmosphere for several hours are shown in Fig. 3. A pentacene coverage of 1.05 ML, with an almost closed first monolayer, is formed in coexistence with some second monolayer nuclei. Figure 3(a) shows an image in an area where the island nuclei have not completely closed up, and the substrate is accessible. A first layer thickness of 2.4–2.5 nm is observed, which is illustrated by the line scan in Fig. 3(b). The AFM tip penetrates the water layer on top of the pentacene since the meniscus force of the water produces an attractive force on the tip.^{18,19} Therefore, the measured step height corresponds to the distance from the substrate surface to the top of pentacene monolayer. This value can be compared with the average value of the step height estimated from the x-ray results tabulated in Table I (curves 2–7), which is 2.4 ± 0.2 nm. The AFM studies also show that the second layer step height is 1.6 ± 0.1 nm, which agrees with the d spacing of the thin film phase of pentacene (1.54 nm). Thus the AFM and x-ray results lead to a consis-

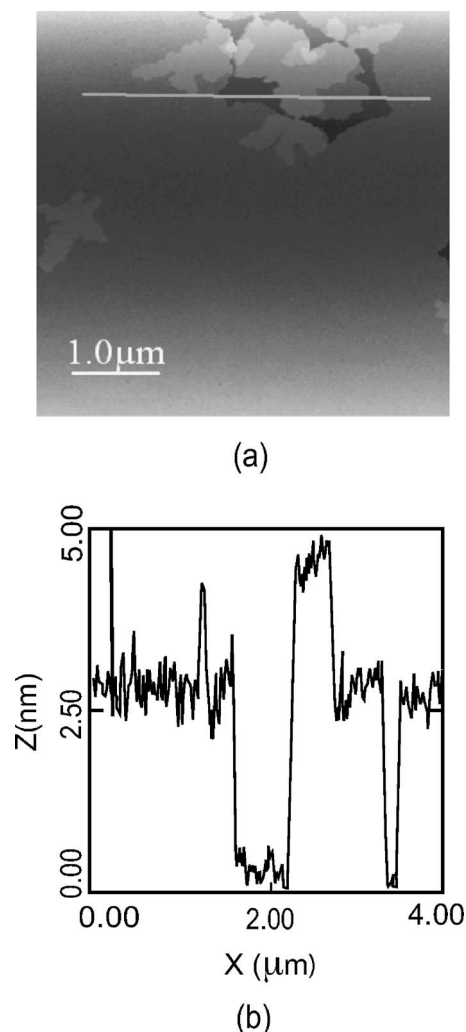


FIG. 3. (a) AFM data taken from the same sample after exposure to atmosphere for several hours. An almost closed first monolayer is formed in coexistence with some second monolayer nuclei. The region in the image shows an area where the island coalescence is not complete. (b) A line scan through the image shows that the first layer step height is about 2.4–2.5 nm. The second layer step height is also shown, which is approximately 1.6 nm.

tent model of pentacene monolayer films, where the first layer height includes the layer of trapped water at the interface.

AFM measurements reported in the literature yield a value of the step height of the pentacene first monolayer of 1.6–1.9 nm.^{15,20,21} These measured step heights do not agree with our value of 2.4–2.5 nm, and the difference in the measured values is difficult to reconcile, although a large uncertainty in the data is inherent to the measurement due to noise in the data. We have also occasionally obtained smaller values for the step height, and we believe that our observations of a reduced step height are due to a compression of the pentacene monolayer by the AFM tip. Estimates of the pressure required to bend the pentacene monolayer and push the interfacial water out of the way show that it is of the same order of magnitude as the pressure that the AFM tip typically applies the surface.^{22,23} A systematic search for this type of effect was conducted using contact mode AFM, and we did not find evidence for compression of the pentacene monolayer by the AFM tip due to the force applied *normal* to the

TABLE II. The measured mobility of two pentacene transistors, one with an OTS treated substrate and one with an untreated substrate. The charge mobilities at atmospheric pressure and in a vacuum environment are compared for each device. Both pentacene layers were deposited at 60 °C.

Ambient pressure (Torr)	Charge mobility, untreated substrate (cm ² /V s)	Charge mobility, OTS treated substrate (cm ² /V s)
760	0.052	0.090
2.0×10^{-6}	0.073	0.112

layer. However, we did find that the measured step height was reduced under conditions where a large *frictional force* was applied. This finding confirms that tip-induced effects are possible under certain imaging conditions. We note that this observation is not directly relevant to most of the literature values of the pentacene monolayer step height, since they are predominantly performed in tapping mode, which does not produce a significant frictional force.

In order to investigate the influence of the interfacial water on the electronic properties of the SiO₂/pentacene interface, we have measured the mobility of two pentacene transistors: one with an untreated SiO₂ gate oxide and another with an OTS treated SiO₂ layer. In addition, we compare results for vacuum and atmospheric pressure environments (both at 25 °C). The mobilities are listed in Table II. The OTS treatment produces a device with improved mobility relative to the untreated device, in agreement with earlier studies.^{5,6} A clear effect was observed, which is consistent with the idea that OTS retards the formation of a water layer, and thus the OTS treated devices do not suffer from the electronic traps caused by water at the interface.⁷ We note that in preliminary x-ray studies, we have not been able to identify a water layer on OTS treated substrates, which also supports this idea. Table II shows that the charge mobility is improved under vacuum conditions for both of the devices. Since our x-ray studies show that the vacuum environment does not significantly reduce the interface moisture, we infer that any increase of the mobility upon exposure to the vacuum environment is not caused by a change in the interface moisture. Rather, it seems likely that the cause of the change of mobility is related to adsorbed gases or moisture at the grain boundaries within the pentacene layer.

IV. CONCLUSIONS

In this article, *in situ* synchrotron x-ray scattering and *ex situ* AFM were used to probe the structure of a deposited pentacene monolayer and the role of water. Reflectivity measurements reveal that there is an adsorbed layer between the pentacene and SiO₂, which is initially present on the substrate and is trapped at the interface when the pentacene film is deposited, even when the substrate is held at an elevated temperature. A water layer also forms on top of the pentacene monolayer after it is exposed to water vapor either from atmosphere or after sufficient exposure in vacuum. The thickness of the water layer on the free surface changes sig-

nificantly under different conditions, but the interfacial water thickness does not.

Transistor *I-V* measurements show that a large change in mobility is observed under conditions that do not produce a significant change in the moisture at the interface. In future studies, it will be interesting to compare single-crystal films (no grain boundaries) with polycrystalline films to see if the sensitivity to environmental conditions can be varied.

ACKNOWLEDGMENTS

We thank Lan Zhou for performing additional AFM measurements to confirm the results reported here and Jie Yang for helpful discussions. We also thank Paul Fenter for checking the x-ray fitting results with a model-independent method. The National Science Foundation supported this work under Award No. DMR-0348354. CHESS is supported by the National Science Foundation and the National Institutes of Health/National Institute of General Medical Sciences under Award No. DMR-0225180. This work was also supported by the CCMR, a Materials Research Science and Engineering Center of the National Science Foundation (DMR-9632275).

- ¹C. D. Dimitrakopoulos and P. R. L. Malenfant, *Adv. Mater.* (Weinheim, Ger.) **14**, 99 (2002).
- ²Z. T. Zhu, J. T. Mason, R. Dieckmann, and G. G. Malliaras, *Appl. Phys. Lett.* **81**, 4643 (2002).
- ³R. Ruiz, A. Papadimitratos, A. C. Mayer, and G. G. Malliaras, *Adv. Mater.* (Weinheim, Ger.) **17**, 1795 (2005).
- ⁴A. C. Mayer, R. Ruiz, R. L. Headrick, A. Kazimirov, and G. G. Malliaras, *Org. Electron.* **5**, 257 (2004).
- ⁵Y. Y. Lin, D. J. Gundlach, S. F. Nelson, and T. N. Jackson, *IEEE Electron Device Lett.* **18**, 606 (1997).
- ⁶H. Klauk, M. Halik, U. Zschieschang, G. Schmid, W. Radlik, and W. Weber, *J. Appl. Phys.* **92**, 5259 (2002).
- ⁷C. Goldmann, D. J. Gundlach, and B. Batlogg, *Appl. Phys. Lett.* **88**, 063501 (2006).
- ⁸R. L. Headrick, G. G. Malliaras, A. C. Mayer, A. K. Deyhim, and A. C. Hunt, *AIP Conf. Proc.* **708**, 1150 (2004).
- ⁹D. L. Windt, *Comput. Phys.* **12**, 360 (1998).
- ¹⁰Y. S. Chu, T. E. Lister, W. G. Cullen, H. You, and Z. Nagy, *Phys. Rev. Lett.* **86**, 3364 (2001).
- ¹¹Z. Zhang, P. Fenter *et al.*, *Langmuir* **20**, 4954 (2004).
- ¹²L. F. Scatena, M. G. Brown, and G. L. Richmond, *Science* **292**, 908 (2001).
- ¹³S. I. Mamatkulov and P. K. Khabibullaev, *Langmuir* **20**, 4756 (2004).
- ¹⁴D. Schwendel, T. Hayashi, R. Dahint, A. Pertsin, M. Grunze, R. Steitz, and F. Schreiber, *Langmuir* **19**, 2284 (2003).
- ¹⁵R. Ruiz, B. Nickel, N. Koch, L. C. Feldman, R. F. Haglund, A. Kahn, and G. Scoles, *Phys. Rev. B* **67**, 125406 (2003).
- ¹⁶R. B. Campbell, J. M. Robertson, and J. Trotter, *Acta Crystallogr.* **14**, 705 (1961).
- ¹⁷C. C. Matheus, A. B. Dros, J. Baas, A. Meetsma, J. L. de Boer, and T. T. M. Palstra, *Acta Crystallogr., Sect. C: Cryst. Struct. Commun.* **57**, 939 (2001).
- ¹⁸J. Jang, G. C. Schatz, and M. A. Ratner, *Phys. Rev. Lett.* **92**, 085504 (2004).
- ¹⁹D. L. Sedin and K. L. Rowlen, *Anal. Chem.* **72**, 2183 (2000).
- ²⁰S. E. Fritz, S. M. Martin, C. D. Frisbie, M. F. Ward, and M. F. Toney, *J. Am. Chem. Soc.* **126**, 4084 (2004).
- ²¹L. Chen, O. Cherniavskaya, A. Shalek, and L. E. Brus, *Nano Lett.* **5**, 2241 (2005).
- ²²L. F. Drummy, P. K. Miska, and D. C. Martin, *J. Mater. Sci.* **39**, 4465 (2005).
- ²³J. N. Israelachvili, *Intermolecular and Surface Forces: With Applications to Colloidal and Biological Systems* (Academic, Boston, MA, 1985), Chap. 13.